Microgravity Science and Technology (2018) 30:877–883
https://doi.org/10.1007/s12217-018-9647-0

ORIGINAL ARTICLE

Experimental Investigation of Buoyant Laminar Jet Diffusion Flames in an Inverted Configuration

Dan Li[1,2] · Shuangfeng Wang[1,2] · Qiang Wang[3]

Received: 31 March 2018 / Accepted: 2 August 2018 / Published online: 18 August 2018

Abstract

Buoyant laminar jet diffusion flames are studied experimentally in an inverted configuration, where gaseous fuel-stream jets vertically downward into air. Flame shape, thermal structure, soot and stability behaviors are obtained until the blowoff limit is reached. By comparing with conventional jet flames, which are established when the fuel jets upward, the effects of buoyancy on laminar diffusion flames are analysed. Downward flame yields larger flame height, although the non-dimensional flame height increases linearly with the Reynolds number at nozzle exit, which is similar to upward flame. Possible reasons for the increased flame height include flow deceleration within downward buoyant flames and presence of more combustion products surrounded the jet stream, thus slowing mixing process between fuel and air. The different relative directions of buoyant flows and jet streams also result in different temperature distributions in downward and upward flames, and a stagnant interface produced by the balance between buoyant flow and jet stream is particularly observed downstream of downward flame. Downward flames contain more soot and the soot formation region is wider, which are mainly attributed to the modifications of flow field and soot path. In addition, downward and upward flames stabilize at different axial positions relative to the nozzle exit. Because of increased characteristic flame residence time, downward flames have higher blowoff limits. The downward jet flame provides an alternative configuration to upward jet flame in studying buoyant diffusion flames due to the different manifestations of buoyancy effects.

Keywords Laminar diffusion flame · Buoyancy · Flame structure · Soot behavior

Introduction

Laminar gaseous jet diffusion flames, which are generally considered as model flame systems to seek a fundamental understanding of complex turbulent diffusion flames, have been studied extensively since the classical work of Burke and Schumann (1928). In most of the studies, a diffusion flame is examined at normal gravity level in a conventional configuration such that the fuel-stream jets vertically upward into air (Hottle and Hawthorne 1949; Roper 1977; Lyons 2007). Because buoyant flow is inherent in combustion processes with effect of gravity, buoyant diffusion flames are a practical flame configuration that is studied on earth. The intrusion of buoyancy poses a crucial question to laminar jet flames, since the jet velocity is relatively small. In particular, the effects of buoyancy raise additional difficulties in experiments and their interpretation, and more problematically may result in flame behaviors that are not relevant to most turbulent flames, which are usually accompanied by large flow velocities. This observation has motivated microgravity experiments of laminar diffusion flames to eliminate effects of buoyancy in the past decades (Bahadori et al. 1993; Faeth et al. 2001; Sunderland et al. 2004, 2008). Investigations on characteristics of non-buoyant laminar jet diffusion flames have shown that flame structures and soot properties are

This article belongs to the Topical Collection: Approaching the Chinese Space Station - Microgravity Research in China
Guest Editors: Jian-Fu Zhao, Shuang-Feng Wang

✉ Shuangfeng Wang
sfwang@imech.ac.cn

[1] Key Laboratory of Microgravity, Institute of Mechanics, Chinese Academy of Sciences, Beijing 100190, China

[2] School of Engineering Science, University of Chinese Academy of Sciences, Beijing 100049, China

[3] School of Automotive and Transportation Engineering, Hefei University of Technology, Hefei, Anhui 230009, China

significantly different from that of buoyant flames. Non-buoyant flames are much taller (up to twice) and wider (up to four times in diameter) than buoyant flames (Haggard and Cochran 1972; Edelman et al. 1973; Edelman and Bahadori 1986; Sunderland et al. 2004). Moreover, Soot pathlines of the buoyant and non-buoyant flames are quite different (Urban et al. 1998). Non-buoyant flames contain more soot and the soot formation region is much wider (Sunderland et al. 1995; Urban et al. 1998). Ma et al. (2015) investigated methane air coflow diffusion flame at normal- and micro-gravity environments both experimentally and numerically. A non-buoyant flame was found to be sootier than its buoyant counterpart by a factor of 4 approximately. The maximum temperature of non-buoyant flame is about 200 K lower than buoyant flame. The maximum axial velocity of non-buoyant flame is reduced to 45% of buoyant flame. Bhowal and Mandal (2016, 2017) investigated methane/air diffusion flame numerically under several gravity conditions. It was shown that the region of peak soot concentration moves towards the jet axis and the mean diameter of soot particle decreases as the gravity level increases.

As far as buoyancy effects are concerned, conventional upward-jet flame at normal gravity and jet flame at microgravity represent two special limiting cases, in which buoyancy-induced convection takes the same direction as the jet stream, and the buoyancy is minimized, respectively. Microgravity experiments, despite of the limited quantity and quality of the experimental results obtained so far, reveal new behaviors that have spurred the reconsideration of laminar diffusion flame. Moreover, comparisons of flame behaviors in these two environments have produced some hints about the effects of buoyancy. However, the test time provided by ground-based microgravity facilities such as drop towers is limited, thus the flame is unsteady during the available test times (Lin and Faeth 1999). On the other hand, opportunities of conducting space-based experiments and results that can be obtained are limited. Consequently, understanding effects of buoyancy on flames needs more investigations. There is another jet flame configuration at normal gravity, where the fuel jet is vertically downward. In this case, buoyant flow has the opposed direction with jet stream, but for upward flame, the two have a same direction. Therefore, in comparison with upward flame, downward flame can provide a valuable configuration in studying buoyancy effects.

In this work, experiments of downward- and upward-jet laminar diffusion flames are conducted to acquire results of flame shape, thermal structure, soot and stability behaviors. Effects of buoyancy on laminar jet diffusion flames are investigated by comparing to the two flame configurations.

Experiments

A schematic illustration of the experimental installation is shown in Fig. 1. It consists of a gas supply system, a gas jet burner, and a measurement and data-acquisition system. The burner is made of a stainless steel tube with an inner nozzle diameter of 1 mm and a length of 120 mm to ensure a fully developed flow at the nozzle exit. Two sets of experiments were conducted, one involving vertically downward injection of fuel into air and resulting in a so-called downward diffusion flame, and the others looking at

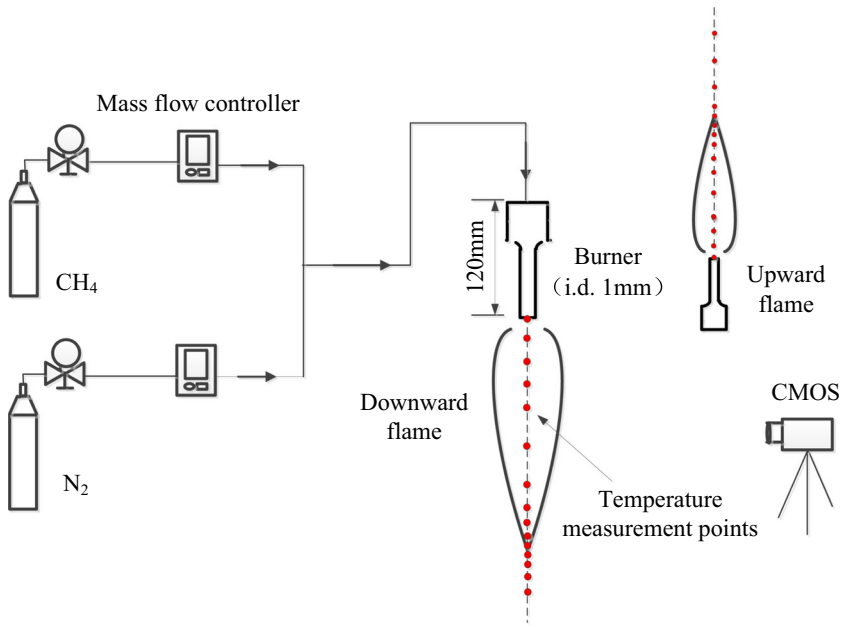

Fig. 1 Experimental setup

vertically upward fuel-jet flames. The fuel is a mixture of methane (purity >99.5%) and nitrogen (purity >99.95%) with a volume ratio of 1:1. The gases are introduced from compressed gas cylinders and are fully mixed before channeling into the nozzle. The gas flow rates are controlled by mass flow controllers (Alicat Scientific) with an accuracy of ±1%. For the downward flame, the mass flow rate of fuel ranges from 0.2 to 0.7 g/min, and the Reynolds number at jet exit ($Re = U_0 d/\upsilon$, where U_0 is the mean velocity at jet exit, d, the inner diameter of fuel nozzle, and υ, the kinematic viscosity of methane-nitrogen mixture) is from 253 to 885. The maximum Reynolds number occurs when the flame exhibits blowoff. The kinematic viscosity of fuel mixture is calculated using the software tool developed by Colorado State University (http://navier.engr.colostate.edu/code/code-2/index.html). For the upward flame, the mass flow rate of fuel ranges from 0.2 to 0.4 g/min, and the Reynolds number is from 253 to 506. The fuel jet is ignited by a torch.

Direct and shadow photographs of flames are captured by a digital camera (Point Grey Research, GS3-U3-41C6C-C) with 4,000,000 pixels, and the framing rate is 90 fps. The visible flame height, h_f, determined from direct flame images, is defined as the distance from the flame base to the flame tip. The error on the measured flame height is mainly due to the uncertainty of flame boundary measurements, and the maximum relative error is estimated to be ±5%.

A Pt-Pt/13% Rh bare wire thermocouple (OMEGA) with a diameter of 50 μm is used to measure the temperatures in the flame. With the help of an electric control translation stage, the thermocouple is individually located at prescribed measurement points, which are schematically shown in Fig. 1. The location accuracy of the thermocouple is ±0.1 mm, and the relative error for the temperature is estimated to be less than ±0.25% in the reported values.

Results and Discussion

Flame Appearance

Photographs of upward jet flames for various Reynolds numbers, *Re*, are shown in Fig. 2, and the one shown in Fig. 2f is captured with a longer exposure time for clearly exhibiting the flame contour. Also indicated in Fig. 2, 'z' and 'r' are the axial and radial coordinates, respectively, with the center of nozzle exit defined as the origin, and the positive direction defined as upward. As seen in Fig. 2a-e, the luminous flame height increases with increasing *Re*, but the variation of flame width is not obvious. A small zone near the flame tip exhibits diluted yellow, and blue flame luminosity encompasses the yellow region, which can be clearly seen from Fig. 2f. So it is clear that soot does not influence the upward flame boundary.

Figure 3 shows images of downward flames for various Reynolds numbers. The flame height increases with the increase of *Re*, which is similar to the upward flame. Different from upward flames, however, the downward flame gradually becomes thinner as *Re* increases. The flame exhibits dark blue and yellow from upstream to downstream, and the yellow region is relatively large, indicating notable soot production in the flame. Actually, a certain amount of soot is observed to emit from the downward flame when $Re<506$. Moreover, at relatively small flow rates, the flame tip turns back towards the burner as shown in Fig. 3a and b.

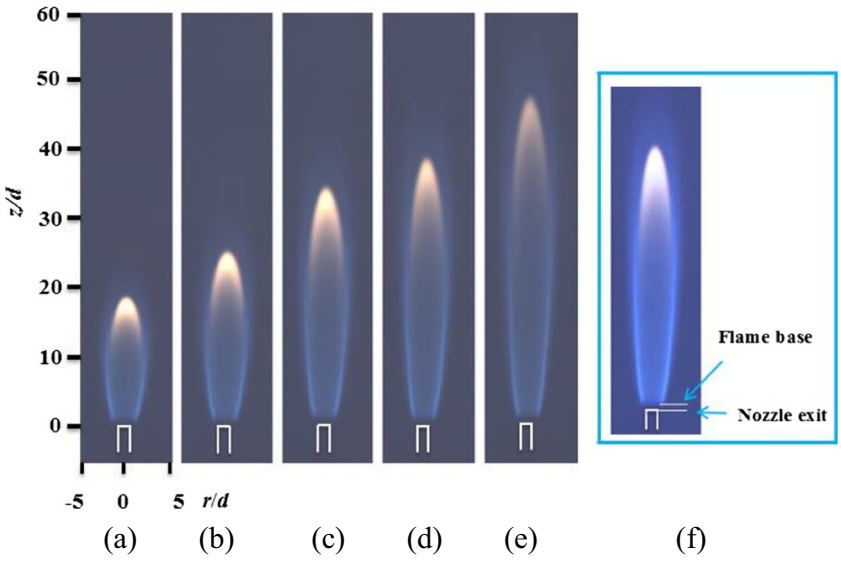

Fig. 2 Upward jet flame images at various Reynolds numbers: **a** $Re = 253$; **b** $Re = 304$; **c** $Re = 379$; **d** $Re = 430$; **e** $Re = 506$; **f** flame image with longer exposure time for $Re = 430$

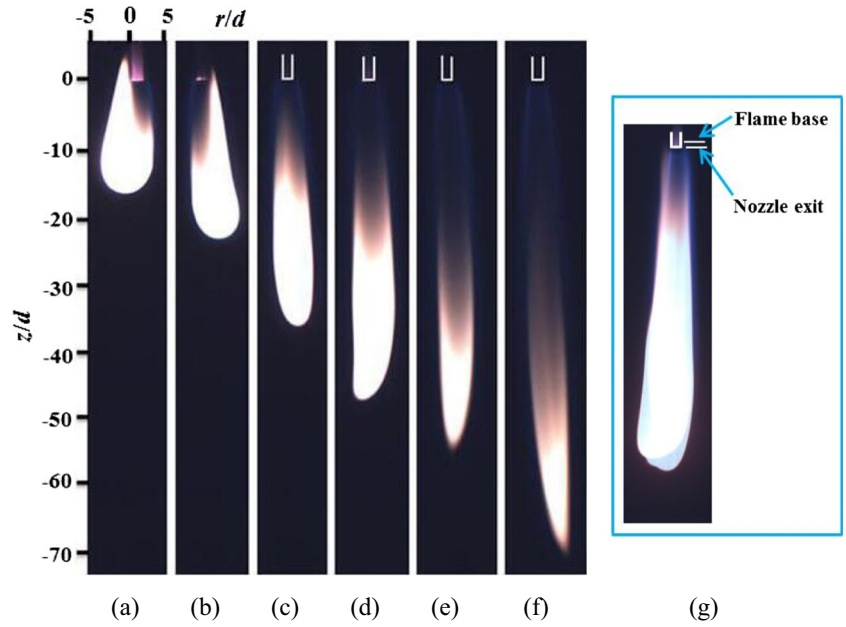

Fig. 3 Downward jet flame images at various Reynolds numbers: **a** $Re = 253$; **b** $Re = 304$; **c** $Re = 379$; **d** $Re = 430$; **e** $Re = 506$; **f** $Re = 632$; **g** flame image with longer exposure time for $Re = 430$

By comparing Fig. 2f with Fig. 3g, it is obvious that the soot region of a downward flame is much larger. The upward flame is axisymmetric and exhibits pencil-like shape at the tip, while the downward flame is not completely axisymmetric and its tip tends to become blunt. In addition, the attachment states of the two flames are different. The upward flame base remains attached above the jet exit, with an axial separate distance of about 1 mm. However, the downward flame base is located at some distance upstream of the nozzle exit.

Flame Shapes and Thermal Structure

The laminar non-premixed flame shape is usually characterized by its visible height (Kent 1986; Urban et al. 1998), and the flame height changes with the gravity level due to buoyancy effects (Edelman et al. 1973; Lin et al. 1999; Aalburg et al. 2005). Luminous flame height are measured from the recorded flame images, and the data for upward and downward flames are plotted in Fig. 4 as a function of *Re* (the blowoff point is denoted by 'B.O.'). Similar to upward flames, non-dimensional flame heights of downward flames are proportional to the Reynolds number. The downward flame is shorter than the corresponding upward flame when $Re<330$. This is mainly caused by the phenomenon that the flame tip turns back towards the burner (see Fig. 3a and b). However, when $Re>330$, a downward flame yields larger flame height. It is well known that buoyancy accelerates the flow within upward flame (Urban et al. 1998). In contrast, buoyant flow takes the opposite direction to the jet stream in downward flame, thus the flow is decelerated. Consequently, the mixing process between fuel and air is slower for downward flame than that for upward flame. Furthermore, accumulation of combustion products around downward flame hinders the transport of air to the flame sheet. It is the slower mixing process that results in the increased flame height for a downward flame.

Shadow photographs of upward and downward flames at $Re = 405$, superposed on the corresponding luminous flames, are shown in Fig. 5. For the upward flame, a high temperature plume region extends downstream for a long distance. Downstream of the downward flame, however, the high temperature region is rather narrow, and its boundary manifests a stagnant interface produced by the balance between buoyant flow and jet stream downstream of the flame tip. Such an interface is particularly observed for

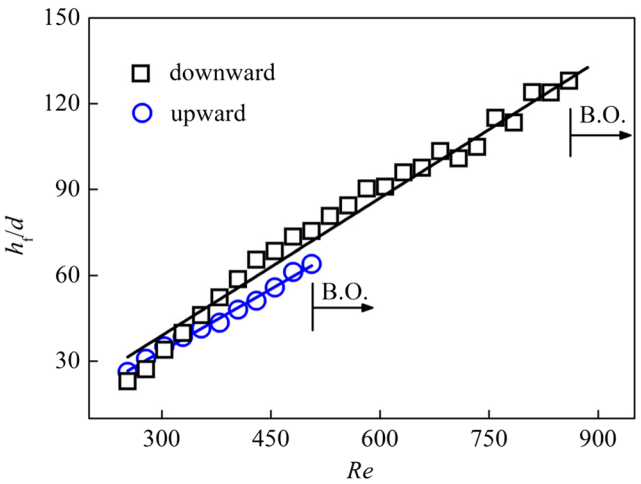

Fig. 4 Luminous flame heights of upward and downward jet flames as a function of Reynolds number. The blowoff limits are denoted by B.O.

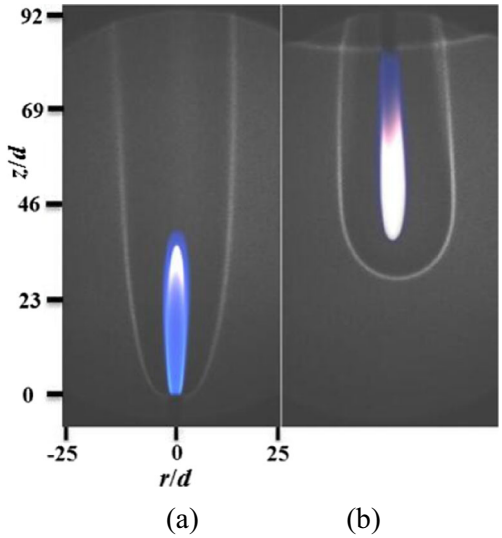

Fig. 5 Shadow photographs of upward and downward flames at $Re = 405$: **a** upward flame; **b** downward flame

downward flame because of the opposed buoyant flow against the jet stream. It is also noted that in downward flame the high temperature plume could preheat the fuel stream at jet exit.

Gas temperatures along the flame axis are plotted in Fig. 6. Both for downward and upward flames, the temperatures increase with distance from the nozzle exit until a maximum is reached near the flame tip ($|z|/h_f = 1.0$). Below the flame tip, the temperature of downward flame is higher than that of upward flame. While the peak temperature of downward flame is lower about 50 K. A more remarkable difference illustrated in Fig. 6, however, is the temperature distribution beyond the visible flame boundary ($|z|/h_f > 1.0$). For downward flames, the temperature drops sharply and reaches the ambient temperature (300 K) approximately at $|z|/h_f = 1.2$. In contrast, the temperature decrease is much more gradual for upward flames, with a measured value of about 1700 K being obtained at $|z|/h_f = 1.2$. These observations are consistent with the corresponding plume properties of downward and upward flames, which are manifested by the photographs in Fig. 5.

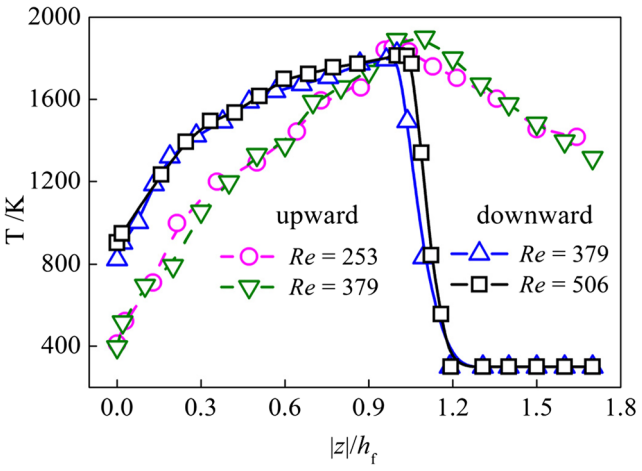

Fig. 6 Centerline temperature distribution in upward and downward flames at Re=379

Soot Processes

There is a direct correlation between soot concentration and flame brightness. The more soot is contained in a diffusion flame, the brighter the flame is. Therefore the flame brightness can be used to qualitatively characterize the line-of-sight integrated soot concentration through the flame (Lin et al. 1999; Aalburg et al. 2005; Abdelgadir et al. 2017). This is also the theoretical basis for soot volume fraction and temperature measurements by two-color imaging method (Stasio and Massoli 1994). Since the brightness of an image is generally represented by the gray values, it is reasonable to investigate relative soot contents within diffusion flames by employing the gray value distribution of flame images.

Typical radial soot distributions in downward and upward flames, characterized by normalized gray values of flame images, are illustrated in Fig. 7. Most soot in the relatively lower part of the flame (about $|z| \leq 40$ mm) is seen to present in an annular region. It is obvious that soot concentration in downward flame is much greater. Meanwhile, soot containing region is wider and longer in downward flame. Gray values increase in a cross section to the maximum near

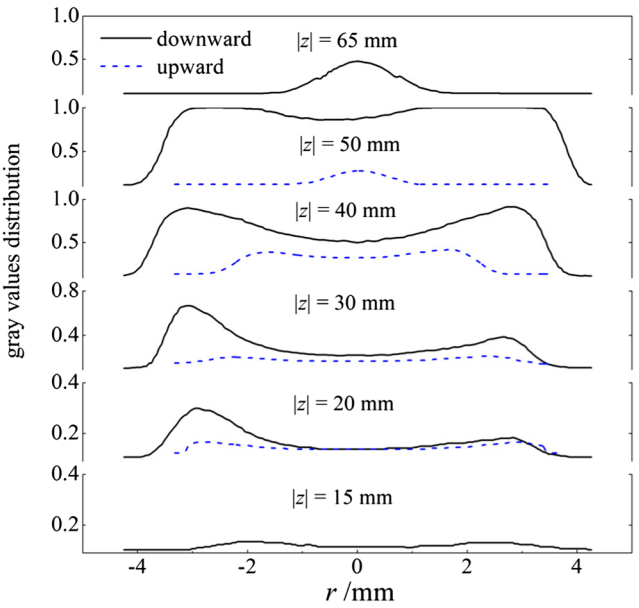

Fig. 7 Radial distributions of normalized gray values of flame image at various axial distances ($Re = 430$)

50 mm ($|z|/h_f = 0.77$) and 45 mm ($|z|/h_f = 0.9$) for downward and upward flames, respectively. The maximum radial distance of gray value profiles for the downward flame is 8.5 mm ($r/d = 8.5$), and for the upward flame is 6.0 mm ($r/d = 6.0$). In addition, the first axial positions of gray values for downward and upward flames are about 15 mm ($|z|/h_f = 0.23$) and 20 mm ($|z|/h_f = 0.4$), respectively. These observations indicate that more soot is contained in downward flames.

In diffusion flames, soot formation regions lie where fuel equivalence ratios (φ) are in the range of 1 to 2 (Sunderland et al. 1995), and soot particles are convected at local flow velocities because the diffusion of soot is relatively small. As illustrated in Fig. 8, where soot formation regions, typical streamlines and soot paths are plotted, soot behaviors in downward and upward flames are very different. Within upward flames, streamlines move inwards to the flame axis due to flow acceleration; within downward flames, however, streamlines move away from the flame axis due to flow deceleration. It is found that for the upward flame soot mainly nucleates in the vicinity of the flame sheet (φ=1), and moves towards positions where fuel equivalence ratios are relatively large (Urban et al. 1998). In contrast, soot within downward flames mainly nucleates inside the inner boundary of formation zone, and then moves across the formation zone. Such soot pathline is a feature similar to those in non-buoyant (microgravity) diffusion flames. After soot nucleation, soot particles experience growth or oxidation in the process of motion with local flow. Soot formation time in downward flames is longer than upward flames, which indicates that more soot is contained in downward flames.

Flame Stability

Under the present experimental conditions all diffusion flames remain attached near the jet exit. As mentioned above, however, the attachment points of downward and upward flames are different. Attachment Points of the upward flame separate from the nozzle exit. However, attachment points of the downward flame are located at upstream of the nozzle exit. For downward flames, buoyant flow has the opposed direction with jet stream, promoting fuel gases to move upward towards the burner. But for upward flames, buoyant flow prevents fuel gases from diffusing the burner.

The upward flame blowoff occurs when jet exit velocity U_0 reaches 8.5 m/s, however, the downward flame blowoff occurs when $U_0 = 14.9$ m/s. Contrary to upward flames, in which the flow accelerates, flow velocities within downward flames decrease with increasing streamwise distance, resulting in longer characteristic flame residence time. Consequently, downward flames have higher blowoff limits.

Concluding Remarks

Downward jet diffusion flames, in which fuel gas jets downward vertically into air, are investigated experimentally. Characteristics of flame shape, thermal structure, soot and stabilization are obtained. Effects of buoyancy on laminar diffusion flames are analyzed by comparing the downward flames with upward flames.

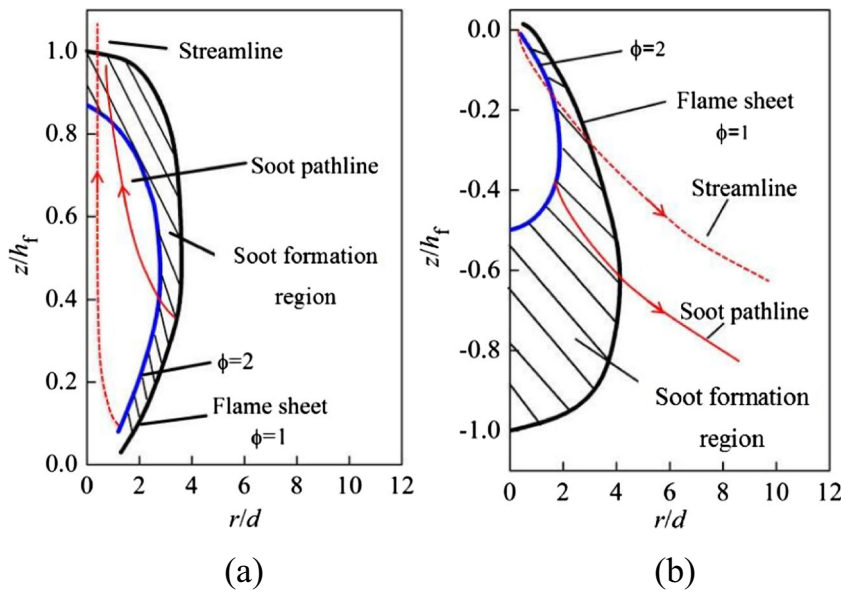

Fig. 8 Sketches of soot formation regions, streamlines, and soot pathlines in upward and downward flames: **a** upward flame; **b** downward flame

It is found that downward flames have larger flame height, and the non-dimensional flame height increases linearly with the Reynolds number at nozzle exit, which is a similar trend for upward flames. Contrary to upward flames, the flow decelerates within downward buoyant flames, and more combustion products are present around the jet stream. Thus the mixing process between fuel and air is slower than that in upward flames, resulting in larger flame heights. The relative different directions of buoyant flows and jet streams also result in different temperature distributions in downward and upward flames, and a stagnation interface near downward flame tip produced by balance between buoyant motion and jet stream is particularly observed. Downward flames contain more soot and soot formation region is wider mainly due to the modifications of flow field and soot path. In addition, the axial position of flame base relative to nozzle exit of downward flame is different from that of upward flame. The longer characteristic flame residence time makes downward flames have higher blowoff limits.

Because of the different manifestations of buoyancy effects, the downward jet flame provides an alternative configuration to upward jet flame in studying buoyant diffusion flames.

Acknowledgments The work is supported by the Strategic Pioneer Program on Space Science, Chinese Academy of Sciences, under Grant No. XDA15007602. The assistant of Ms. Feng Zhu in preparation of the manuscript is also acknowledged.

References

Aalburg, C., Diez, F.J., Faeth, G.M., Sunderland, P.B., Urban, D.L., Yuan, Z.G.: Shapes of nonbuoyant round hydrocarbon-fueled laminar-jet diffusion flames in still air. Combust. Flame **142**, 1–16 (2005)

Abdelgadir, A., Rakha, I.A., Steinmetz, S.A., Attili, A.: Effects of hydrodynamics and mixing on soot formation and growth in laminar coflow diffusion flames at elevated pressures. Combust. Flame **181**, 39–53 (2017)

Bhowal, A.J., Mandal, B.K.: A computational study of soot formation in methane air co-flow diffusion flame under microgravity conditions. Microgravity. Sci. Technol. **28**, 395–412 (2016)

Bhowal, A.J., Mandal, B.K.: Numerical simulation of transient development of flame, temperature and velocity under reduced gravity in a methane air diffusion flame. Microgravity. Sci. Technol. **29**, 151–175 (2017)

Burke, S.P., Schumann, T.E.W.: Diffusion flames. Ind. Eng. Chem. **20**, 998–1004 (1928)

Bahadori, M.Y., Stocker, D.P., Vaughan, D.F., Zhou, L., Edelman, R.B.: Effects of buoyancy on laminar, transitional, and turbulent gas jet diffusion flames. In: Willams, F.A., Oppenheim, A.K., Olfe, D.B., Lapp, M. (eds.) Modern Developments in Energy Combustion & Spectroscopy, pp. 49–66. Pergamon Press, New York (1993)

Edelman, R.B., Fortune, O.F., Weilerstein, G., Cochran, T.H., Haggard, J.B.: An analytical and experimental investigation of gravity effects upon laminar gas jet-diffusion flames. Proc. Combust. Inst. **14**, 399–412 (1973)

Edelman, R.B., Bahadori, M.Y.: Effects of buoyancy on gas-jet diffusion flames: experiment and theory. Acta Astronaut. **13**, 681–688 (1986)

Faeth, G.M., Urban, D.L., Yuan, Z.G.: Laminar and turbulent gaseous diffusion flames. In: Ross, H.D. (ed.) Microgravity Combustion: Fire in Free Fall. Academic Press, San Diego (2001)

Haggard, J.B., Cochran, T.H.: Stable hydrocarbon diffusion flames in a weightless environment. Combust. Sci. Technol. **5**, 291–298 (1972)

Hottle, H.C., Hawthorne, W.R.: Diffusion in laminar flame jets. Proc. Combust. Inst. **3**, 254–265 (1949)

Kent, J.H.: A quantitative relationship between soot yield and smoke point measurements. Combust. Flame **63**, 349–358 (1986)

Lyons, K.M.: Toward an understanding of the stabilization mechanisms of lifted turbulent jet flames: experiments. Prog. Energy. Combust. Sci. **33**, 211–231 (2007)

Lin, K.C., Faeth, G.M.: Shapes of nonbuoyant round luminous laminar-jet diffusion flames in coflowing air. AIAA J. **37**, 759–765 (1999)

Lin, K.C., Faeth, G.M., Sunderland, P.B., Urban, D.L., Yuan, Z.G.: Shapes of nonbuoyant round luminous hydrocarbon/air laminar jet diffusion flames. Combust. Flame **116**, 415–431 (1999)

Ma, B., Cao, S., Giassi, D., Stocker, D.P., Takahashi, F., Bennett, B.A.V., Smooke, M.D., Long, M.B.: An experimental and computational study of soot formation in a co-flow jet flame under microgravity and normal gravity. Proc. Combust. Inst. **35**, 839–846 (2015)

Roper, F.G.: The prediction of laminar jet diffusion flame sizes: Part I. Theoretical model. Combust. Flame **29**, 219–226 (1977)

Satio, K., Williams, F.A., Gordan, A.S.: Effects of oxygen on soot formation in methane diffusion flames. Combust. Sci. Technol. **47**, 117–138 (1986)

Stasio, S.D., Massoli, P.: Influence of the soot property uncertainties in temperature and volume-fraction measurements by two-colour pyrometry. Meas. Sci. Technol. **5**, 1453–1465 (1994)

Sunderland, P.B., Köylü, Ü.Ö., Faeth, G.M.: Soot formation in weakly buoyant acetylene-fueled laminar jet diffusion flames burning in air. Combust. Flame **100**, 310–322 (1995)

Sunderland, P.B., Krishnan, S.S., Gore, J.P.: Effects of oxygen enhancement and gravity on normal and inverse laminar jet diffusion flames. Combust. Flame **136**, 254–256 (2004)

Sunderland, P.B., Haylett, J.E., Urban, D.L., Nayagam, V.: Lengths of laminar jet diffusion flames under elevated gravity. Combust. Flame **152**, 60–68 (2008)

Urban, D.L., Yuan, Z.G., Sunderland, P.B., Linteris, G.T., Voss, J.E., Lin, K.C., Dai, Z., Sun, K., Faeth, G.M.: Structure and soot properties of nonbuoyant ethylene/air laminar jet diffusion flames. AIAA J. **36**, 1346–1360 (1998)